Simplified crossover droplet model for adsorption of pure fluids in slit pores

S. B. Kiselev[a] and J. F. Ely
Chemical Engineering Department, Colorado School of Mines, Golden, Colorado 80401-1887

(Received 25 November 2003; accepted 12 January 2004)

We present a generalized crossover (GC) model for the excess adsorption of pure fluids at a flat solid–liquid interface, which reproduces scaling behavior of the excess adsorption in the critical region and is reduced to the classical, van der Waals-type analytical model far away from the bulk critical point. In developing this model, we used the density-functional theory (DFT) approach for the order parameter profile calculations with a generalized corresponding states model for the local free-energy density. The GC DFT model well represents the available experimental adsorption data for Kr/graphite, C_2H_4/graphite, C_3H_8/graphite, CO_2/silica, and SF_6/graphite systems in the entire density range $0<\rho\leqslant 3\rho_c$ and temperatures up to $1.7T_c$. In the critical region $0.5\rho_c<r\leqslant 1.5\rho_c$ and $T\leqslant 1.15T_c$, the GC DFT model is consistent with the predictions of the asymptotic renormalization-group crossover model for the critical adsorption in a semi-infinite system developed earlier. For the excess adsorption on the critical isochore, both theories predict a scaling-law behavior $\Gamma\propto\tau^{-\nu+\beta}$, but fail to reproduce a ''critical depletion'' of the excess adsorption along the critical isochore of the SF_6/graphite system near T_c. We show that an anomalous decrease of adsorption observed in this system at $\tau=T/T_c-1<10^{-2}$ can be explained by finite-size effect and develop a simplified crossover droplet (SCD) model for the excess adsorption in a slit pore. With the effective size of the pore of $L=50$ nm, the SCD model reproduces all available experimental data for SF_6/graphite, including the critical isochore data where $\tau\to 0$, within experimental accuracy. At $L\gg\xi_b$ (where ξ_b is a bulk correlation length) the SCD model is transformed into the GC DFT model for semi-infinite systems. Application of the SCD model to the excess adsorption of carbon dioxide on the silica gel is also discussed. © *2004 American Institute of Physics.* [DOI: 10.1063/1.1665507]

I. INTRODUCTION

Understanding of phase transitions and surface phenomena at the solid–fluid and liquid–fluid interfaces, such as physical adsorption and wetting, is of fundamental importance in many practical processes.[1] The analytical, classical Langmuir, Brunauer–Emmett–Teller, and local density theories[2,3] give reasonable representations of the adsorption data far away from the critical point. However, all these theories fail to reproduce the nonanalytical singular behavior of the adsorption in the critical region. We also note that the simplified engineering local density model,[4–7] based on the empirical Peng–Robinson equation of state, cannot correctly reproduce the thermodynamic surface of pure fluids in the critical region. More rigorous integral equation approaches[8,9] also fail in the critical region, because the equations cannot be closed.

In order to describe the nonanalytical singular behavior of the excess adsorption in the critical region, more rigorous renormalization-group (RG) theory models should be considered. A RG crossover model for the critical adsorption of fluids on a planar interface has been developed recently by Kiselev *et al.*[10] This RG model is based on the general field-theoretical approach for the systems under the second-order phase transition described with the Landau–Ginzburg–Wilson (LGW) effective Hamiltonian with the scalar order parameter and can be applied to systems such as pure fluids and fluid mixtures, ionic solutions, polymers, and polymer blends. However, this model is essentially an asymptotic crossover model, which is valid only in the extended critical region where the long-wavelength fluctuations of the order parameter are big enough to be treated with the LGW effective Hamiltonian. This is not a case for the dilute-gas and dense-fluid regimes. Therefore, the RG model, which provides a smooth crossover of the excess adsorption Γ from the scaling, $\Gamma\propto\tau^{-\nu+\beta}$, at $|\tau|\ll$Gi to the mean-field, $\Gamma\propto\log\tau$, behavior at Gi$\ll|\tau|<1$ (here Gi is a Ginzburg number) in the critical region, cannot be extrapolated to the dilute-gas and dense-liquid regions. Another shortcoming of the crossover RG model of Kiselev and co-workers[10] is that it was formulated only for semi-infinite systems and in its present form cannot be applied to the analysis of the critical adsorption in a confined geometry such as a cylindrical capillary or slit pore.

As the critical point of bulk fluid is approached, the excess adsorption of a fluid in a slit pore drastically differs from the adsorption in the bulk volume. The effect of the confined geometry on the critical adsorption of sulfur hexafluoride (SF_6) in a colloidal graphitized carbon black and a mesoporous controlled-pore glass has been studied by

[a]Author to whom correspondence should be addressed. Fax: (303) 273-3730. Electronic mail: skiselev@mines.edu

Thommes and co-workers.[11–13] They found that at temperatures well above criticality ($10^{-2} \leqslant \tau \equiv T/T_c - 1 \ll 1$), in agreement with the scaling hypothesis formulated by Fisher and de Gennes,[14] the excess adsorption diverges along the critical isochore as $\Gamma \propto \tau^{-\nu+\beta}$ ($\nu - \beta \cong 0.3$). However, on approaching the critical point (at $\tau \simeq 10^{-2}$) the temperature dependence of the adsorption exhibits reentrance and Γ decreases sharply as $\tau \to 0$, contrary to theoretical predictions.[14] The first attempts to address this problem were made by Schoen and Thommes,[15] Maciolek and co-workers,[16,17] and Wilding and Schoen.[18] Similar to the original works of Thommes *et al.*,[11–13] the critical depletion of Γ in Refs. 15–18 was also attributed to the effect of confined geometry on the near-critical fluid, but no physically self-consistent explanation for the sharp decrease of the adsorption at $\tau \to 0$ has been proposed. In all these studies, in accordance with the earlier theoretical prediction by Marconi,[19] the excess adsorption along the critical isochore in a slit pore monotonically increases and eventually saturates as the critical temperature is approached. That led the authors of Ref. 17 to the conclusion that the sharp decrease of Γ cannot be accounted for by a single pore model.

Kiselev and co-workers[20,21] proposed another interpretation of the critical depletion, without considering finite-geometry effects. It was shown that the anomalous decrease of the adsorption along the critical isochore can be successfully treated by supposing that the surface-order parameter vanishes linearly with τ, corresponding to an *ordinary* surface phase transition.[22–24] However, this result contradicts the conclusion reached by Upton,[25] who has argued that a fluid against a hard wall belongs to the universality class of *normal* surface phase transitions, as introduced by Fisher.[26] As was shown in our previous work,[10] in the case of vanishing surface ordering field, the theory fails to reproduce the experimental excess adsorption isotherms at $|\tau| < 10^{-2}$. Therefore, we conclude that this interpretation of the reentrant behavior of the critical adsorption observed experimentally[11–13] should be ruled out. Thus, so far, no theoretical crossover model for the excess adsorption of fluids in semi-infinite systems and slit pores has been developed.

In this work, we continue the study initiated in our previous work on the excess adsorption[10] and interfacial properties[27] of pure fluids in and beyond the critical region. Here we develop a generalized crossover (GC) model for the excess adsorption of pure fluids on the solid–liquid interface in a semi-infinite system, which is similar to the recently developed generalized crossover model for the thermodynamic and liquid–vapor interfacial properties for pure fluids.[27] In developing the GC model for the excess adsorption we use a combination of the above-mentioned field-theoretical approach[10] with density-functional theory (DFT) for the interfacial phenomena.[3,28] Using simple scaling arguments, we incorporate the confined-geometry effects into the GC model, thereby developing a simplified crossover droplet model for the excess adsorption for a semi-infinite system and in a slit pore. The model was tested against experimental excess adsorption data for Kr/graphite, C_2H_4/graphite, C_3H_8/griphite, CO_2/silica, and SF_6/graphite systems.

We proceed as follows: In Sec. II we review the density-functional theory results for the surface tension and excess adsorption. In Sec. III we describe a generalized crossover model for the Helmholtz free energy and the surface tension and provide comparisons with experimental data for Kr, C_2H_4, and CO_2. The generalized crossover model for the excess adsorption in a semi-infinite system and its comparison with experimental data are presented in Sec. IV. The simplified crossover droplet model for the excess adsorption in a slit pore is considered in Sec. V. Our results are summarized in Sec. VI.

II. DENSITY-FUNCTIONAL THEORY

The surface excess, or Gibbs, adsorption of pure fluids on a planar surface in a semi-infinite system is defined as

$$\Gamma = \int_0^\infty [\rho(z) - \rho_b] dz, \tag{2.1}$$

where $\rho(z)$ is density of fluid at a distance z from the surface and $\rho_b = \rho(\infty)$ is the bulk density of the fluid. The density profile $\rho(z)$ can be found from optimization of the functional[3]

$$\mathcal{F}[\rho(z)] = \int [\hat{A}(\rho) + c_0 (\nabla \rho)^2 + W_s(\rho)] dV, \tag{2.2}$$

where $\hat{A}(\rho) = \rho A(T,\rho)$ is a Helmholtz free-energy density of the bulk fluid and $W_s(\rho)$ is the surface contribution into the free energy density. Optimization of the functional (2.2) by Langrange's method leads to the Euler–Lagrange equation

$$\frac{d\Delta\hat{A}(\rho)}{d\rho} - 2c_0 \frac{d^2\rho}{dz^2} + \frac{dW_s(\rho)}{d\rho} = 0, \tag{2.3}$$

where $\Delta\hat{A}(\rho) = \hat{A}(T,\rho) - \hat{A}(T,\rho_b) - (\rho - \rho_b)\mu(T)$ is the excess part of the free-energy density and $\mu(T) = \mu(T,\rho_b) = (\partial\hat{A}/\partial\rho)_T|_{\rho=\rho_b}$ is the chemical potential of the bulk fluid. In the field-theoretical approach,[22–24] the surface contribution can be presented in the form

$$W_s = b_1 \delta(z) m_1^2 - h_1 \delta(z) m_1, \tag{2.4}$$

where b_1 is a surface constatnt, $\delta(z)$ is the Kronecker symbol, $h_1(\tau)$ is a surface ordering field, and $m_1 = \rho_1/\rho_c - 1$ is a surface order parameter. The first integral of Eq. (2.3) can be written in the form

$$\frac{d\rho}{dz} = \pm \frac{1}{\sqrt{c_0}} [\Delta\hat{A}(\rho) + W_s]^{1/2}, \tag{2.5}$$

where signs "+" and "−" correspond to the increasing and decreasing density profile, respectively. For the excess adsorption, the minimum of the functional $\mathcal{F}[\rho(z)]$ corresponds to the negative sign in Eq. (2.5) with the boundary conditions in the volume (at $z \to \infty$),

$$\rho(z \to \infty) = \rho_b, \quad \left(\frac{d\rho}{dz}\right)_{z\to\infty} = \left(\frac{d^2\rho}{dz^2}\right)_{z\to\infty} = 0, \tag{2.6}$$

and at the surface (at $z \to 0$),

$$\rho(z \to 0) = \rho_1,$$

$$2c_0\left(\frac{d\rho_1}{dz}\right)=2c_0\left(\frac{d\rho}{dz}\right)_{z\to 0}=(2b_1m_1-h_1)\rho_c^{-1}. \tag{2.7}$$

Using the boundary condition (2.7) in Eq. (2.5), one can obtain an equation of state (EOS) for the surface order parameter m_1 or for the surface density $\rho_1=(m_1+1)\rho_c$ in the form

$$4c_0\Delta\hat{A}(\rho_1)=(2b_1m_1-h_1)^2\rho_c^{-2}, \tag{2.8}$$

which provides a relationship between the surface ordering field h_1 and surface density ρ_1 at any fixed values of the temperature T and bulk density ρ_b. The temperature dependence appears in Eq. (2.8) through the excess free-energy density $\Delta\hat{A}(\rho_1)$, surface ordering field h_1, and parameters b_1 and c_0. In Eq. (2.8) the parameter $b_1=b_{10}\sqrt{c_0k_BT}$, while the surface field can be represented at $|\tau|<1$ by truncated Taylor expansion,[10]

$$\frac{h_1(\tau)}{\sqrt{c_0k_BT_c}}=h_{10}+\sum_{i=1}h_{1i}\tau^i, \tag{2.9}$$

where h_{1i} are the system-dependent coefficients, while for the parameter c_0 a good approximation is[27]

$$c_0=(1-\kappa_0)^2k_BT_c\rho_c^{-2/3}, \tag{2.10}$$

where k_B is Boltzmann constant and $\kappa_0<1$ is a system-dependent parameter which takes into account a difference of the prefactor $(1-\kappa_0)$ in real fluids from unity.

In the general case, Eqs. (2.5) and (2.8) for the density profile $\rho(z)$ can be solved only numerically, which makes calculation of the excess adsorption with Eq. (2.1) rather complicated. However, if one is not interested in the actual density profile, it is useful to rewrite Eq. (2.1) in the form

$$\Gamma=\int_0^\infty(\rho(z)-\rho_b)dz=\int_{\rho_1}^{\rho_b}(\rho(z)-\rho_b)\left(\frac{d\rho}{dz}\right)^{-1}d\rho. \tag{2.11}$$

Substituting Eq. (2.5) into Eq. (2.11) we then find for the adsorption

$$\Gamma=\int_{\rho_1}^{\rho_b}\frac{(\rho-\rho_b)}{[\Delta\hat{A}(\rho)]^{1/2}}d\rho, \tag{2.12}$$

which can be integrated numerically without calculation of the density profile $\rho(z)$.

The surface tension on the planar liquid–vapor interface is defined in the density functional theory as[3,29]

$$\sigma=2\int_{-\infty}^{+\infty}c_0\left(\frac{\partial\rho}{\partial z}\right)^2dz, \tag{2.13}$$

where $\rho(z)$ is density profile between vapor, $\rho_V=\rho(z\to-\infty)$, and liquid, $\rho_L=\rho(z\to+\infty)$, phases. Similar to the adsorption, the density profile in Eq. (2.13) is also described by Eq. (2.5), but with zero surface energy $W_s(\rho)\equiv 0$ and free-energy density for the vapor–liquid interface, $\Delta\hat{A}(\rho)=\hat{A}(T,\rho)-\hat{A}(T,\rho_V)-(\rho-\rho_V)\mu(T)$, where $\mu(T,\rho_{V,L})=(\partial\rho A/\partial\rho)_T$ is a chemical potential of the bulk fluid along the saturated curve $\rho=\rho_{V,L}(T)$. The final expression for the surface tension can be written in the form[27]

$$\sigma=c_0^{1/2}\int_{\rho_V}^{\rho_L}[\Delta\hat{A}(\rho)]^{1/2}d\rho. \tag{2.14}$$

In order to calculate the excess adsorption and surface tension with Eqs. (2.12) and (2.14), respectively, one needs to specify the Helmholtz free energy $A(T,\rho)$, the coefficient κ_0, and the surface constants b_{10} and h_{1i} $(i=0,1,2,...)$.

III. EQUATION OF STATE AND SURFACE TENSION

In this work, for the Helmholtz free energy of a bulk fluid we use a generalized corresponding states (GCS) model presented in our previous paper.[27] A general crossover expression for the dimensionless Helmholtz free energy $\overline{A}(T,v)=A(T,v)/RT$, where R is the gas constant, in the GCS model is written in the form[27]

$$\overline{A}(T,v)=\Delta\overline{A}(\overline{\tau},\overline{\eta})-K(\tau,\eta)-\Delta v\overline{P}_0(T)+\overline{A}_0^{res}(T)+\overline{A}_{id}(T), \tag{3.1}$$

where the critical part of the Helmholtz free energy

$$\Delta\overline{A}(\overline{\tau},\overline{\eta})=\overline{A}^{res}(\overline{\tau},\overline{\eta})-\overline{A}_0^{res}(\overline{\tau})-\ln(\overline{\eta}+1)+\overline{\eta}\overline{P}_0(\overline{\tau}), \tag{3.2}$$

$K(\tau,\eta)$ is the kernel term, $\overline{A}^{res}$ is the dimensionless residual part of the free energy corresponding to the reference classical EOS, $\overline{P}_0(T)=P(T,\rho_{0c})/\rho_{0c}RT$ and $\overline{A}_0^{res}(T)=\overline{A}^{res}(T,\rho_{0c})$ are the dimensionless pressure and residual part of the free energy along the critical isochore $\rho=\rho_{0c}$, respectively, and $\overline{A}^{id}(T)$ is the dimensionless temperature-dependent ideal-gas Helmholtz free energy. In Eqs. (3.1) and (3.2), the renormalized dimensionless temperature deviation $\overline{\tau}$ and order parameter $\overline{\eta}$ are given by

$$\overline{\tau}=\tau\Upsilon^{-\alpha/2\Delta_1},$$
$$\overline{\eta}=\eta\Upsilon^{(\gamma-2\beta)/4\Delta_1}+(1+\eta)\Delta v_c\Upsilon^{(2-\alpha)/2\Delta_1}, \tag{3.3}$$

where $\alpha=0.11$, $\beta=0.325$, $\gamma=2-2\beta-\alpha=1.24$, and $\Delta_1=0.51$ are universal nonclassical critical exponents,[30,31] $\Upsilon(\tau,\eta)$ denotes a crossover function, $\eta=v/v_c-1$ is a dimensionless deviation of the molar volume $v=1/\rho$ from the real critical molar volume $v_c=1/\rho_c$, and $\Delta v_c=(v_c-v_{0c})/v_{0c}\ll 1$ is a dimensionless shift of the critical volume v_c with respect to the classical value $v_{0c}=1/\rho_{0c}$ obtained from the reference classical equation on state used for calculating $\overline{A}^{res}(T,v)$.

In the GCS model,[27] the kernel term $K(\tau,\eta)$, which is responsible for the asymptotic singular behavior of the isochoric heat capacity along the critical isochore, was set equal to zero, while for the reference EOS a simple cubic Patel–Teja (PT) EOS (Refs. 32 and 33) has been chosen. The explicit form of the crossover function $\Upsilon(\tau,\eta)$ and functions $\overline{A}^{res}(T,v)$, $\overline{A}_0^{res}(T)$, and $\overline{P}_0(T)$ for the PT EOS can be found in Ref. 27. All system-dependent parameters in the GCS model are expressed as functions of the Pitzer's accentric factor ω, real compressibility factor $Z_c=P_c/\rho_cRT_c$, and molecular weight M_w. The EOS $P(v,T)=-(\partial A/\partial v)_T$ for the GCS model can be written in the dimensionless form

$$P_r=f_{PT}^{cr}(T_r,\rho_r;\omega,Z_c), \tag{3.4}$$

TABLE I. System-dependent constants for the GCS EOS.

	T_c (K)	ρ_c (mol l^{-1})	Z_c	ω	M_w
Krypton	209.400	10.965	0.288000	0.0	83.800
Ethylene	282.350	7.6372	0.281208	0.0898	28.052
n-propane	369.850	5.0000	0.276247	0.1520	44.097
SF_6	318.690	5.0000	0.283838	0.2100	146.05
CO_2	304.128	10.625	0.274588	0.2250	44.010

where $P_r=P/P_c$, $T_r=T/T_c$, $\rho_r=\rho/\rho_c$, and the function $f_{PT}^{cr}=-RT(\partial A/\partial v)_T/P_c$ is calculated with $A(T,v)$ as given by Eq. (3.1). In order to apply the GCS model to real fluids one needs to know the real critical parameters P_c, T_c, ρ_c, and accentric factor ω for the fluid of interest.

The system-dependent parameters for the GCS EOS for pure krypton, ethylene, *n*-propane, and carbon dioxide, considered in this work, are listed in Table I. A detailed comparison of the GCS model predictions with experimental data for *n*-alkanes and CO_2 was given in our previous work.[27] Therefore, here we will show the GCS model predictions only for krypton (Kr) and ethylene (C_2H_4), which were not considered in Ref. 27. In Fig. 1 we show the predictions of the GCS model in comparison with one-phase experimental *P-V-T* data for ethylene. A comparison of the predictions of the GCS model with the saturated pressure and density data for C_2H_4 and Kr is shown in Figs. 2 and 3. In Fig. 4 we show the predictions of the GCS model for the heat of vaporization for C_2H_4 and Kr together with experimental data. The crosses in Fig. 4 represent the values calculated with a new fundamental EOS for C_2H_4 by Smukala *et al.*[34] As one can see from Figs. 1–4, excellent agreement the GCS model predictions and experimental data for both fluids is observed. Only at temperatures $T<140$ K for ethylene does the GCS model predict systematically lower (up to 4%) values of the heat of vaporization than those calculated with the EOS by Smukala *et al.*,[34] but at higher temperatures both equations give very similar results.

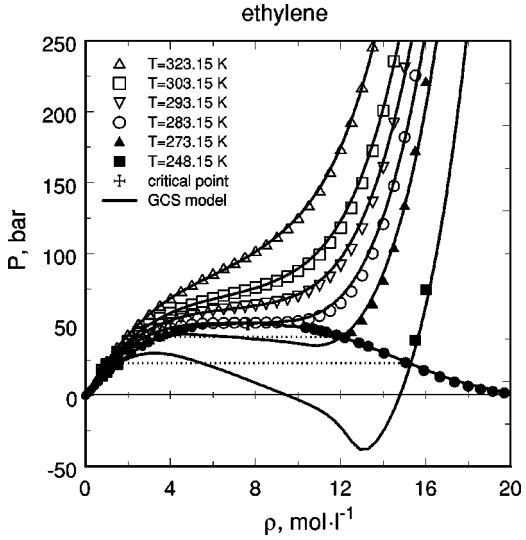

FIG. 1. $P\rho T$ data (symbols) for ethylene (Ref. 47) with predictions of the GCS model (curves).

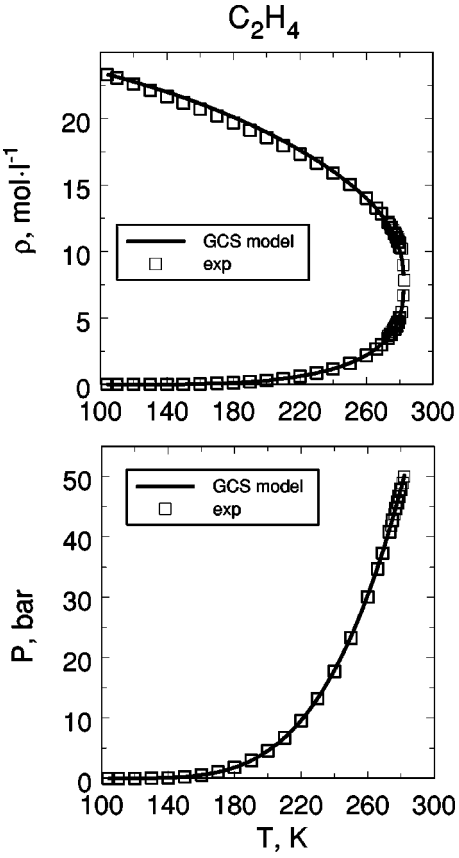

FIG. 2. The saturated density (top) and saturated pressure (bottom) data for ethylene (Ref. 48) (symbols) with predictions of the GCS model (curves).

As we pointed out in our previous paper,[27] the parameter κ_0 can be determined from the experimental surface tension data at $T_r\simeq 0.7$ or calculated with the corresponding states expression

$$\kappa_0=1.194\times 10^{-2}M_w\left[1-\frac{1.91\omega^{1/2}}{(1+0.405\omega)^2}\right], \tag{3.5}$$

which appears to be a good approximation for *n*-alkanes and some other nonionic and nonassociating fluids. For cryogenic fluids a prefactor (1/3) on the right-hand side of Eq. (3.5) should be applied.[27] Equation (3.5) is an entirely empirical correlation and, therefore, it should be used with caution. If any experimental surface-tension data for the fluid of interest are available, it is recommended to test Eq. (3.5) against experimental data.

In Fig. 5 we show a comparison of the prediction of the GCS-DFT model for surface tension with experimental data for CO_2, C_2H_4, and Kr. The solid curves in Fig. 5 represent the values calculated with parameter κ_0 extracted form experimental data and the dashed curves correspond to κ_0 calculated with Eq. (3.5). In Eq. (3.5) for Kr, the prefactor (1/3) has been applied. As one can see, for CO_2 and C_2H_4 both curves practically coincide and they both are in very good agreement with experiments. However, for Kr the GCS-DFT model with the parameter κ_0 calculated with Eq. (3.5), even with the prefactor (1/3), yields systematically lower values of the surface tension as compared to experimental values. With

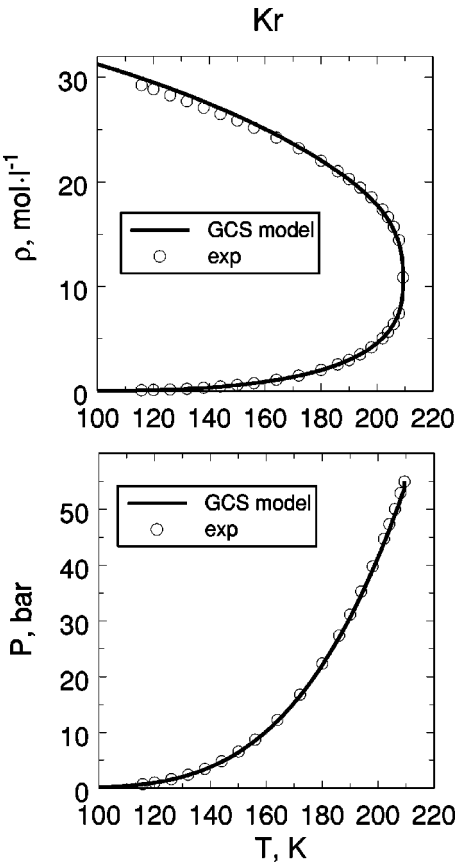

FIG. 3. The saturated density (top) and saturated pressure (bottom) data for krypton (Ref. 49) (symbols) with predictions of the GCS model (curves).

$\kappa_0=\kappa_0^{\text{expt}}$ the GCS-DFT predictions for Kr are in excellent agreement with surface tension experimental data.

IV. EXCESS ADSORPTION

In the asymptotic crossover (AC) RG model developed earlier by Kiselev and co-workers,[10] the excess part of the

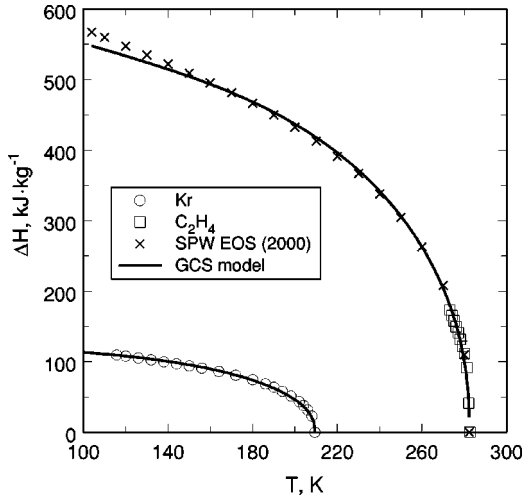

FIG. 4. The heat of vaporization as a function of temperature for ethylene and krypton: Ref. 49 (symbols) with predictions of the GCS model (curves). The crosses represent the values calculated with a new EOS for ethylene by Smukala *et al.* (Ref. 34).

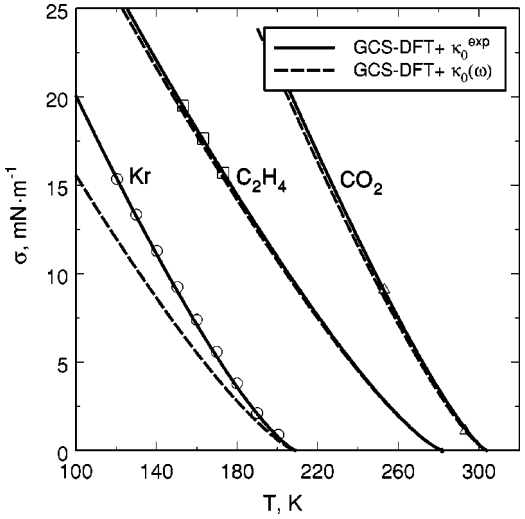

FIG. 5. The surface tension data for carbon dioxide (Ref. 49), ethylene (Ref. 49), and krypton (Ref. 50) (symbols) with predictions of the GCS-DFT model (curves).

Helmholtz free energy density in Eq. (2.2) was considered in the Landau–Ginzburg–Wilson form, which restricts its application to the critical region only. Here, in the generalized crossover for the excess adsorption, named the GC DFT model, for the excess energy $\Delta\hat{A}$ in Eqs. (2.2)–(2.12) we use the GCS model.[27] Since the GCS model[27] incorporates the nonanalytic scaling laws in the critical region and in the limit $\rho\to 0$ reproduces the ideal gas behavior, the GC DFT model developed in this work reproduces the singular behavior of the excess adsorption in the critical region and, unlike the AC RG model,[10] can be also extended to the dilute-gas regime. In order to apply the GC DFT to real physical systems, all system-dependent parameters for the bulk fluid can be taken from the GCS-DFT model, while the surface constants b_{10} and h_{1i} $(i=0,1,2,...)$ should be found from the optimization of the GC DFT excess adsorption data for the system of interest.

The first system which we considered here was krypton on graphitized carbon black studied by Findenegg.[35] For pure krypton we adopt the same GCS parameters as given in Table I, while the surface constants b_{10}, h_{10}, and h_{11} have been found from a fit of the GC DFT model to experimental data.[35] Since for Kr the difference between the parameter κ_0 calculated with Eq. (3.5) and κ_0^{expt} is rather essential, it is interesting to know how the uncertainty in the parameter κ_0 influences the accuracy of representation of the excess adsorption in this system. With this in mind, the constants b_{10}, h_{10}, and h_{11} have been optimized with two different values of the parameter κ_0. The excess adsorption was calculated with Eq. (2.12), where the experimental $T-P$ coordinates were transformed into the $T-\rho$ coordinates [needed in Eq. (2.12)] using the GCS EOS (3.4). We found that for excess adsorption the exact value of the parameter κ_0 in the GC DFT is not crucial, and in both cases, with $\kappa_0=\kappa_0^{\text{expt}}$ and $\kappa_0=\kappa_0(\omega)$, very good agreement between the calculated values and experimental data is observed. This means that, in principle, the parameter κ_0 in the GC DFT can always be estimated with the CS expression (3.5). However, in order to

TABLE II. Surface parameters for the GC DFT model.

	b_{10}	h_{10}	h_{11}	h_{12}
Kr/graphitized carbon[a]	3.876	6.564	−2.414	⋯
C_2H_4/graphitized carbon	6.623	9.861	0.806	⋯
C_3H_8/graphitized carbon	43.08	41.52	−99.51	⋯
SF_6/graphitized carbon	43.44	81.01	−103.8	⋯
CO_2 /C_{18}-silica	1.00	2.30	−12.0	⋯
CO_2/silica gel	1.414	5.121	−6.024	2.690

[a]Parameter $\kappa_0=0.15$ determined from experimental surface tension data.

keep physical self-consistency of the GC DFT model, we have adopted the experimental value $\kappa_0^{\text{expt}}=0.15$. The values of the surface constants for Kr/graphitized carbon and other systems considered in this work are listed in Table II.

A comparison the GC DFT model predictions with the excess adsorption isotherms obtained by Findenegg[35] is shown in Fig. 6. The solid and dashed curves in Fig. 6 represent the values calculated with the simplified local density (SLD) model developed for this system by Subrahanian *et al.*[5] As one can see from Fig. 6, in general the GC DFT model gives better predictions for the excess adsorption, especially at near-critical and supercritical pressures at isotherms $T=253.15$ and 273.15 K, where the SLD model[5] systematically underestimates the experimental excess adsorption.

In Figs. 7 and 8 we show a comparison of the predictions of the GC DFT and SLD model for the excess adsorption of ethylene (Fig. 7) and *n*-propane (Fig. 8) on graphitized carbon black with experimental data by Findenegg.[35] Similar to the previous system, the surface constants b_{10}, h_{10}, and h_{11} in Eq. (2.8) for these systems have been found from the optimization of the GC DFT model to experimental data, but with the parameter κ_0 calculated with Eq. (3.5). As one can see, far away from the critical point (at $P \ll P_c$) both GC DFT and SLD models give very similar results. However, in the critical region the GC DFT yields a more accurate and physically self-consistent representation of the excess adsorption than the SLD by Subrahanian *et al.*[5] This not an unexpected result. As we mentioned before, the SLD model,[4–7] based on the classical Peng–Robinson EOS, in principle cannot reproduce the nonanalytic singular behavior of the excess adsorption in the critical region. Just as the

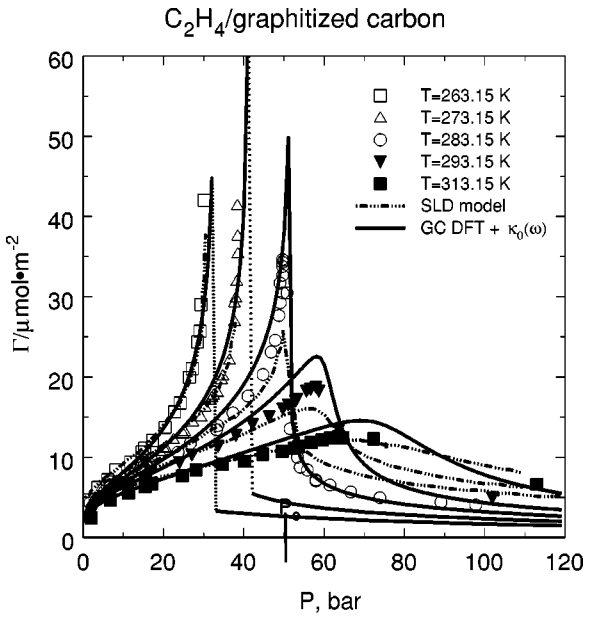

FIG. 7. Surface excess adsorption data (Ref. 35) (symbols) of ethylene on graphitized carbon black as function of pressure. The solid curves represent the values calculated with the GCS-DFT model and the dot-dashed curves correspond to the values calculated with the SLD model (Ref. 5). The dotted lines represent the vapor pressure of pure C_2H_4 calculated at $T=263.15$ and 273.15 K with the GCS EOS.

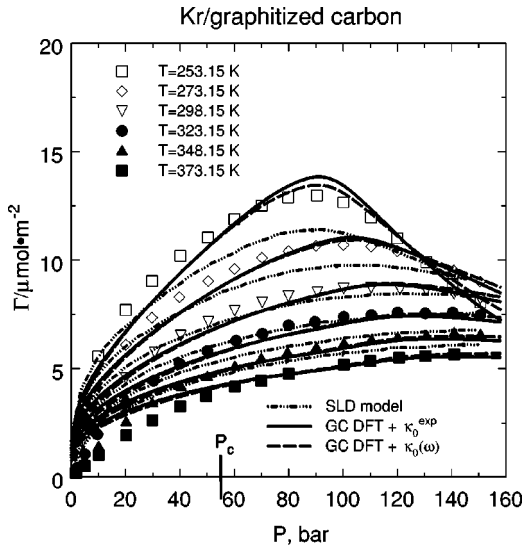

FIG. 6. Surface excess adsorption data (Ref. 35) (symbols) of krypton on graphitized carbon black as function of pressure. The solid and dashed curves represent the values calculated with the GCS-DFT model with different values of the parameter κ_0, and the dot-dashed curves correspond to the values calculated with the SLD model (Ref. 5).

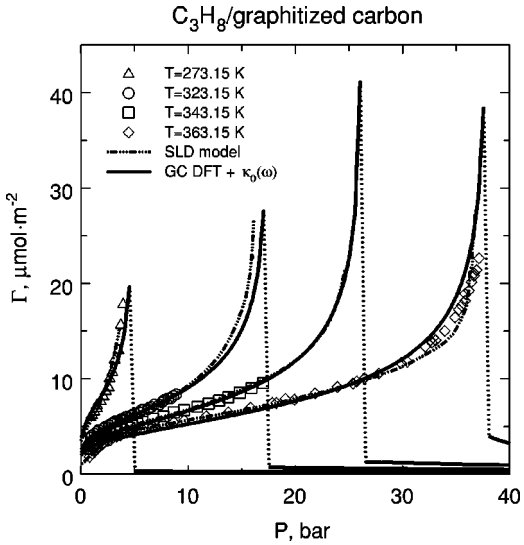

FIG. 8. Surface excess adsorption data (Ref. 35) (symbols) of *n*-propane on graphitized carbon black as a function of pressure. The solid curves represent the values calculated with the GCS-DFT model, the dot-dashed curves correspond to the values calculated with the SLD model (Ref. 5), and the dotted lines represent the vapor pressure of pure C_3H_8 calculated at the same temperatures with the GCS EOS.

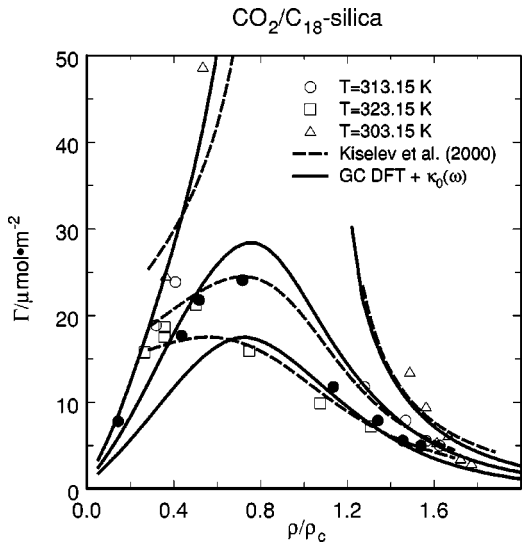

FIG. 9. Surface excess adsorption data (Refs. 36 and 37) (symbols) of carbon dioxide on octadecyl-bounded silica as a function of density. The solid curves the values calculated with the GC DFT model and the dashed curves correspond to the values calculated with the AC RG model by Kiselev *et al.* (Ref. 10).

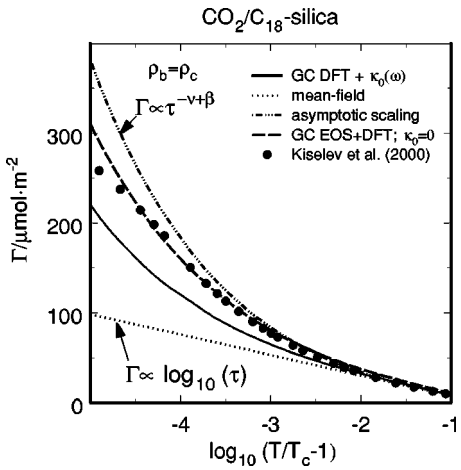

FIG. 10. Surface excess adsorption of CO_2 on octadecyl-bounded silica along the critical isochore as a function of temperature. The symbols correspond to the values generated with the AC RG model by Kiselev *et al.* (Ref. 10), and the solid and long-dashed curves represent the values calculated with the GC DFT model with (Ref. 27) and GC (Ref. 38) equations of state, respectively.

Peng–Robinson EOS gives a singularity for the isobaric heat capacity, the SLD model[4–7] also yields a singularity for Γ, but with wrong classical critical exponent. The GC DFT model, based on the GCS model, not only accurately describes excess adsorption in the regular region of the parameters of state, but also reproduces the theoretically well-established scaling law behavior for the excess adsorption in the critical region.

In order to prove this statement, we considered here the carbon dioxide on octadecyl-bounded silica (C_{18}-silica) substrate, system which was also studied in our previous work.[10] In Fig. 9 we show the excess adsorption isotherms of carbon dioxide on octadecyl-bounded silica as functions of density calculated with the GC DFT model (the solid curves) with the AC RG model[10] (the dashed curves). The open and solid symbols in Fig. 9 represent the two different experimental data sets obtained for this system by Strubinger and Parcher.[36,37] There is an obvious discrepancy between two data sets at $T=313.15\,\mathrm{K}$, but otherwise good agreement between calculated values and experimental data is observed. As one can see from Fig. 9, at densities $0.6\rho_c \leqslant \rho \leqslant 1.6\rho_c$ both the GC DFT and AC RG models give very similar predictions. There are no excess adsorption experimental data for this system along the critical isochore of CO_2. Therefore, in Fig. 10 we show a comparison between the predictions of different theoretical models (the curves) and data generated at the critical isochore with the AC RG model[10] (solid symbols). As one can see, at $10^{-3} < \tau \leqslant 10^{-1}$ the GC DFT and AC RG models practically coincide, but at $\tau < 10^{-3}$ the GC DFT model predicts systematically lower values than those generated with the AC RG model. The reason for this is that for calculating the thermodynamic potential in the GC DFT model we use the GCS EOS with the kernel term $K(\tau,\eta) \equiv 0$ and all system-dependent parameters expressed as empirical functions of ω, Z_c, and M_w. As consequence, in the GC DFT model the critical amplitude Γ_0 (which determines the asymptotic value of the excess adsorption along the critical isochore $\Gamma|_{\rho=\rho_c} = \Gamma_0 \tau^{-\nu+\beta}$) is smaller than in the AC RG model with all system-dependent parameters optimized to experimental data for this system.[10] Better consistency between the GC DFT and AC RG models in the asymptotic critical region can be achieved by using for CO_2 the generalized cubic EOS with a nonzero kernel term and parameters found from a fit of experimental P-V-T and C_P data.[38] In this case (see the dashed curve in Fig. 10), excellent agreement between the GC DFT predictions and the values generated with the AC RG model is observed down to reduced temperatures $\tau = 10^{-4} - 10^{-5}$.

The last system, which we considered in this work, is adsorption of hexafluoride on graphitized carbon black measured by Thommes *et al.*[11] A comparison of the excess adsorption of SF_6 on graphitized carbon black calculated along a few supercritical isotherms calculated with the GC DFT model with experimental data[11] is shown in Fig. 11. Excellent agreement between the values calculated with the GC DFT model and experimental data[11] is observed on all isotherms (from $T=313.18\,\mathrm{K}$ to $T=343.52\,\mathrm{K}$) in the entire density range $0 \leqslant \rho \leqslant 2.0\rho_c$. The dashed curves in Fig. 11 represent the values calculated with the AC RG model.[10] As one can see, in the rage of validity of the AC RG model good agreement between the calculated values and experimental is also observed. However, a completely different scenario appears in Fig. 12, where we show a comparison of the calculated values for the excess adsorption along the critical isochore with experimental values by Thommes *et al.*[11] As one can see, similar to the CO_2/silica system both the GC DFT and AC RG models predict monotonically increasing behavior of the excess adsorption at $T \to T_c$, which at $\tau \to 0$ diverges as $\Gamma \propto \tau^{-\nu+\beta}$, while experimental data exhibit a completely different behavior. The excess adsorption in this system increases only down to a reduced temperature of $\tau \simeq 0.01\,(\Delta T \simeq 2\,\mathrm{K})$, but then Γ decreases sharply on approaching T_c. In principle, experimental data for the excess

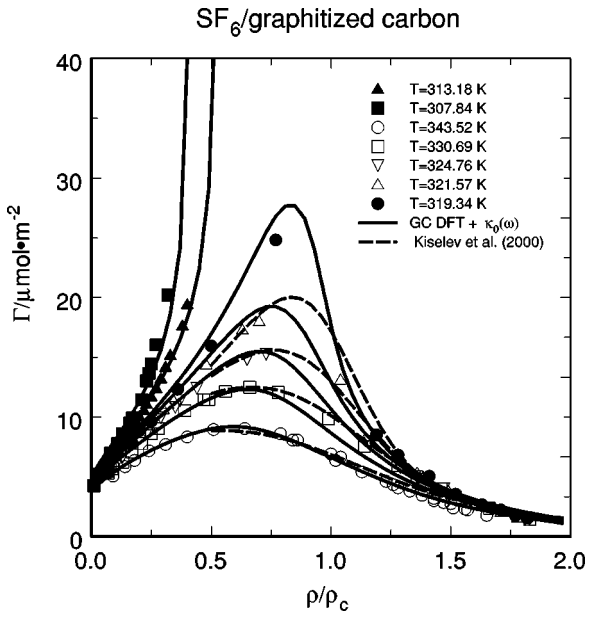

FIG. 11. Surface excess adsorption data (Ref. 11) (symbols) of sulfur hexafluoride on graphitized carbon black as a function of density. The solid curves represent the values calculated with the GC DFT model and the dashed curves correspond to the vales calculated with the AC RG model by Kiselev *et al.* (Ref. 10).

adsorption along the critical isochore for the SF_6/graphitized carbon system[11] can be described with the GC DFT and AC RG models if we assume that the surface parameter $h_{10} \equiv 0$ (see the dotted curve in Fig. 12). But in this case, as was shown in our previous work,[10] the theory fails to reproduce the excess adsorption isotherms shown in Fig. 11. In order to treat properly the anomalous behavior of the excess adsorption observed in experiment,[11] a finite-geometry effect should be incorporated into the GC DFT model for a semi-infinite system.

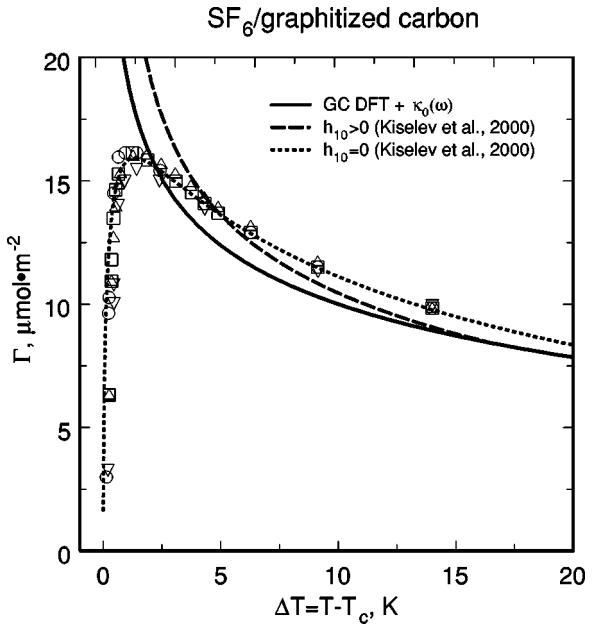

FIG. 12. Surface excess adsorption data (Ref. 11) (symbols) of SF_6 on graphitized carbon black along the critical isochore as a function of temperature. The solid curve corresponds to the values calculated with the GC DFT model, and the dashed and dotted curves represent the values calculated with the AC RG model by Kiselev *et al.* (Ref. 10) with $h_{10} > 0$ and $h_{10} = 0$, respectively.

V. SIMPLIFIED CROSSOVER DROPLET MODEL

In this paper, the effect of finite geometry on the critical adsorption in a slit pore has been incorporated into the GC DFT in a framework of the so-called droplet model of the critical state. In the droplet model, a fluid near the critical point is considered as an ''ideal gas'' of homogeneous liquid droplets with the droplet radius equal to the correlation length of a bulk fluid at a temperature T and density ρ, $r = \xi_b(T,\rho)$.[39,40] The number of droplets, N, in the volume V in this case is proportional to $\propto V/\xi_b^3$ and, consequently, the excess free-energy density

$$\Delta\hat{A} = \frac{Nk_BT}{V} \propto k_BT/\xi_b^3. \tag{5.1}$$

According to the scaling theory of the critical phenomena,[41,42] the correlation length ξ_b and excess free-energy density $\Delta\hat{A}$ can be expressed in the vicinity of the critical point of a fluid as universal scaled functions of the scaled argument $x = \eta/|\tau|^{\beta}$:

$$\xi_b = |\tau|^{-\nu} f_{\xi}(x), \quad \Delta\hat{A} = |\tau|^{2-\alpha} f_A(x). \tag{5.2}$$

Along the critical isochore $f_x(0) = \xi_0$ and $f_A(0) = a_0$, and Eqs. (5.1) and (5.2) lead to the so-called hyperscaling relation $3\nu = 2 - \alpha$ or, in d-dimensional space,

$$d\nu = 2 - \alpha, \tag{5.3}$$

which appears to be more fundamental (for a review see Refs. 30 and 31) than the simple physical arguments which we used here in its derivation. This encouraged us to apply the droplet model for the analysis of the critical adsorption in a slit pore.

The density profile in a slit pore, which physically corresponds to the droplet model given above, is schematically shown in Fig. 13. The solid curve in Fig. 13 corresponds to case 1, when the correlation length is much smaller than the distance between walls in the pore, $\xi_b \ll L/4$. In this case, the density at the center of the pore at $z = l = L/2$ is equal to the density of the bulk fluid at the given temperature and pressure, $\rho_l = \rho_b(T,P)$, and a slit pore is physically equivalent to a semi-infinite system. In case 2, marked in Fig. 13 by the dashed curve, the correlation length is still smaller than L, $\xi_0 \ll \xi_b < L/4$, but the density $\rho_l = \rho(L/2)$ at the center of the pore is not equal to the bulk density ρ_b, $\rho_1 > \rho_l > \rho_b$. The conditions (2.6) in this case should be written in the form

$$\rho(z = L/2) = \rho_l > \rho_b, \quad \left(\frac{d\rho}{dz}\right)_{z=L/2} = \left(\frac{d^2\rho}{dz^2}\right)_{z=L/2} = 0, \tag{5.4}$$

and Eq. (2.12) for the surface excess adsorption in a slit pore should be replaced by

$$\Gamma = \int_{\rho_1}^{\rho_l} \frac{(\rho - \rho_l)}{[\Delta\hat{A}(\rho)]^{1/2}} d\rho. \tag{5.5}$$

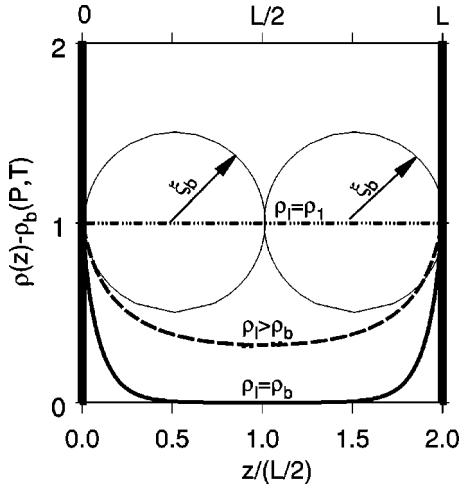

FIG. 13. Schematic representation of the density profile in arbitrary units as a function of the distance from the wall in a slit pore of size L.

In the case when the correlation length $\xi_b \geqslant L/4$, shown in Fig. 13 by the dot-dashed curve, the density ρ_l in Eq. (5.5) becomes very close to the surface density ρ_1 ($\rho_l \to \rho_1$) and, as a consequence, $\Gamma \to 0$. At fixed temperature T, the condition $\xi_b \geqslant L/4$ along the critical isochore $\rho_b = \rho_c$ is achieved at in a slit pore with size $L \leqslant 4\xi_0 \tau^{-\nu}$ or in the pore with a fixed size L at the reduced temperatures $\tau \leqslant (4x_0/L)^{1/\nu}$. Estimation of the characteristic size of the pore with the equation

$$L_c = 4\xi_0 \tau_1^{-\nu}, \tag{5.6}$$

where $\tau_1 = 0.01$ is the reduced reentrant temperature observed in the experiment[11] and $\xi_0 = 0.15-0.2$ nm is a reasonable estimate for pure SF_6,[43] yields $L_c = 50-70$ nm, which is close to the value $L_c = 31$ nm reported by Thommes *et al.*[13] Taking into account the uncertainty in determination of the parameters τ_1, ξ_0, and the characteristic size L_c itself, we contend that this prediction is very good.

In order make predictions using the droplet model for the excess adsorption in a slit pore more quantitative and accurate, one needs to know an explicit dependence of the density ρ_l on L and ξ_b. This function cannot be obtained in the framework of the droplet model by itself, and a more rigorous renormalization-group theory should be used for this purpose. However, the RG equation for the order parameter profile in this case can only be solved numerically, which makes the calculations of the excess in a slit pore with Eq. (5.5) rather complicated. Therefore, in the simplified crossover droplet (SCD) model developed in this work, for this function we chose here a simple phenomenological expression

$$\rho_l = \rho_b - (\rho_b - \rho_1)\tanh\left(\frac{x^2}{1+x}\right), \quad x = 4\xi_b/L, \tag{5.7}$$

which is consistent with the physically obvious boundary conditions for the density in the center of the pore,

$$\rho_l(x \to 0) = \rho_b, \quad \rho_l(x \to \infty) = \rho_1, \tag{5.8}$$

and its first derivatives:

$$\left(\frac{d\rho_l}{dx}\right)_{x\to 0} = \left(\frac{d\rho_l}{dx}\right)_{x\to\infty} = 0. \tag{5.9}$$

The excess adsorption is calculated in the SCD model with Eq. (5.5), where the surface density ρ_1 is determined from the solution of Eq. (2.8) for a semi-infinite system, and for the correlation length in Eq. (5.7) we use the Ornstein–Zernike approximation[41]

$$\xi_b = \sqrt{\frac{c_0 \overline{\chi_T}}{\chi_0^+}}, \tag{5.10}$$

where the parameter c_0 is calculated with Eq. (2.10) and χ_0^+ is the asymptotic amplitude in the power law $\overline{\chi_T}|_{\rho=\rho_c} = \chi_0^+ \tau^{-\gamma}$ for the dimensionless isothermal compressibility $\overline{\chi_T} = \rho T(\partial\rho/\partial P)_T P_c \rho_c^{-2} T_c^{-1}$ along the critical isochore $\rho = \rho_c$ of a bulk fluid at $\tau \to +0$.

To test this model we the excess adsorption of SF_6 on graphitized carbon black experimentally studied by Thommes *et al.*[11] At temperatures $T < T_c$ and $\Delta T \geqslant 5$ K the SCD model predictions for SF_6/graphitized carbon system practically coincide with the values calculated with the GC DFT model and, therefore, are not shown in Fig. 11. The results of our calculations of the excess adsorption in a slit pore with in comparison with experimental data along the separate isochores as a function of temperature obtained for SF_6/graphitized carbon system by Thommes *et al.*[11] are shown in Figs. 14 and 15. The solid curves in Figs. 14 and 15 represent the values calculated with SCD model with $L = 50$ nm and all other parameters as given in Table II. The dot-dashed and dashed curves correspond to the values calculated with the GC DFT and AC RG models the semi-infinite systems, respectively. As one can see, along the critical isochore at $\Delta T \geqslant 5$ K ($\tau \geqslant 0.02$) the excess adsorption calculated with the SCD model coincides with the GC DFT model predictions for a semi-infinite system. However, at $\Delta T \simeq 2$ K, unlike the GC DFT and AC RG predictions, the excess adsorption calculated with the SCD model passes a maximum and, in agreement with experimental data, goes to zero as $T \to T_c$ ($\tau \to 0$). The predictions of the SCD model at other subcritical and supercritical densities are shown in Fig. 15. As one can see from Fig. 15, the predictions of the SCD model at other densities are also in excellent agreement with experimental data. At densities $\rho/\rho_c = 1.2$ and 1.3 the excess adsorption calculated with the SCD model increases only slightly as the saturated temperature $T_s(\rho)$ is approached, while at subcritical densities, at $\rho/\rho_c = 0.7$ and 0.8, Γ increases sharply as $T \to T_s(\rho)$. Agreement between the SCD model and experimental data for noncritical isochores is even better than for the AC RG model,[10] which was specifically optimized for these data.

Another confined system considered here is adsorption of carbon dioxide on the silica gel, which is an adsorbent with a broad pore size distribution ranging from micropores of 0.8 nm to 16 nm. An experimental and theoretical study of this system was presented recently by Mazzotti and co-workers.[44,45] The quantity measured in the experiment[44] was the excess adsorption n^{ex} defined as

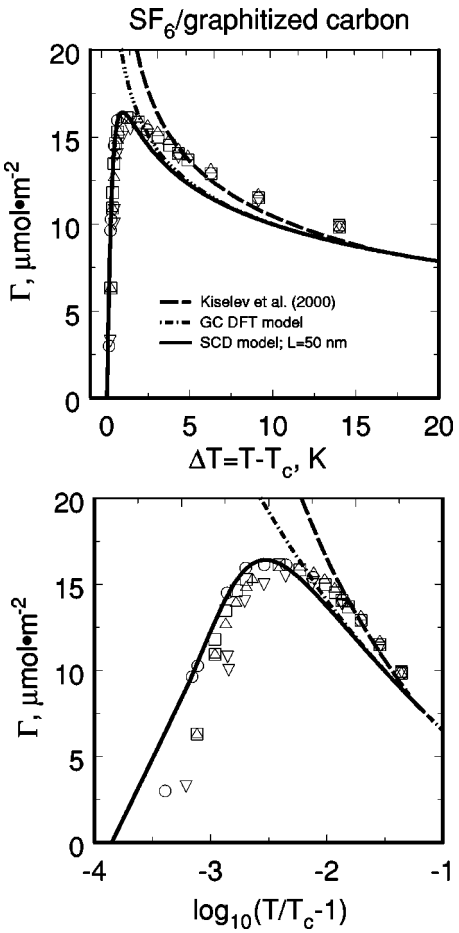

FIG. 14. Surface excess adsorption data (Ref. 11) (symbols) of SF_6 on graphitized carbon black along the critical isochore as a function of temperature in normal (top) and semilogarithmic scale (bottom). The solid curves correspond to the values calculated with the SCD model, the dot-dashed curves represent the GC DFT model predictions, and the dashed curves correspond to the values calculated with the AC RG model by Kiselev *et al.* (Ref. 10).

$$n^{ex}=\frac{1}{m_{sorb}}\int_{V_{\rm tot}}[\rho(\vec{r})-\rho_b]dV$$

$$=\frac{v_{\rm tot}}{V_{\rm tot}}\int_{V_{\rm tot}}[\rho(\vec{r})-\rho_b]dV, \qquad (5.11)$$

where m_{sorb} is the mass of the adsorbent particle with the pore volume $V_{\rm tot}$ and specific pore volume $v_{\rm tot}=V_{\rm tot}/m_{sorb}$. In order to apply the SCD model for calculation of this quantity, one needs to specify the geometry and size distribution of the pores. In this work, silica gel was described as a porous media with one-dimensional slit pores of three different widths L_1 with volume fraction x_{1v}, L_2 with volume fraction x_{2v}, and L_3 with volume fraction $x_{3v}=1-x_{1v}-x_{2v}$. In this case, the excess adsorption n^{ex} can be written in the form

$$n^{ex}=\left[\sum_{i=1}^{3}\left(\frac{2\Gamma_i}{L_i}+\rho_{li}\right)x_{iv}-\rho_b\right]v_{\rm tot}, \qquad (5.12)$$

where Γ_i is the surface excess adsorption in the pore of size L_i calculated with Eq. (5.5). For the specific pore volume $v_{\rm tot}$ and merging pore sizes $L_1=L_{\min}$ and $L_2=L_{\max}$ we adopted the values obtained by Hocher *et al.*,[45]

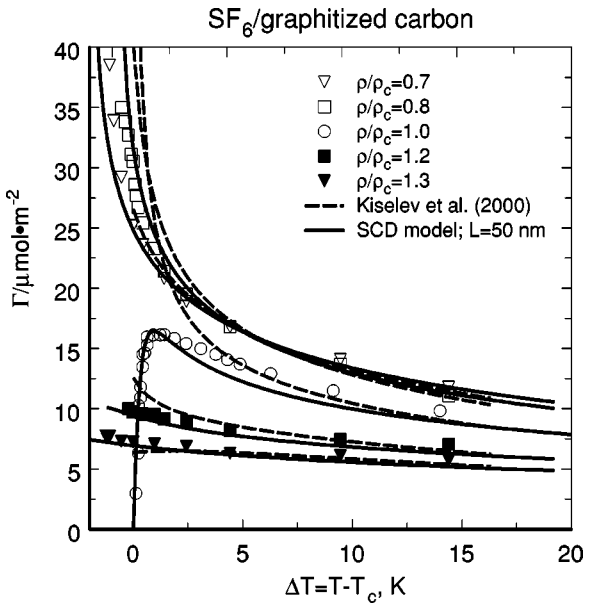

FIG. 15. Surface excess adsorption isochores (Ref. 11) (symbols) of SF_6 on graphitized carbon black as a function of temperature. The solid curves correspond to the values calculated with the SCD model and the dashed curves correspond to the values calculated with the AC RG model by Kiselev *et al.* (Ref. 10).

$$v_{\rm tot}=0.74\ \text{mL/g}, \quad L_1=0.8\ \text{nm}, \quad L_2=16\ \text{nm}, \qquad (5.13)$$

while the parameters

$$x_{1v}=0.040, \quad x_{2v}=0.765, \quad L_3=2.9\ \text{nm}, \qquad (5.14)$$

as well as the surface constants in Eq. (2.8), have been found from the optimization of the SCD model to experimental data. The values of the surface parameters b_{10} and h_{1j} $(j=0-2)$ for this system are listed in Table II.

Comparison of the predictions of the SCD model with experimental data for CO_2/silica gel obtained by Di Giovanni *et al.*[44] is shown in Fig. 16. Since the adsorption iso-

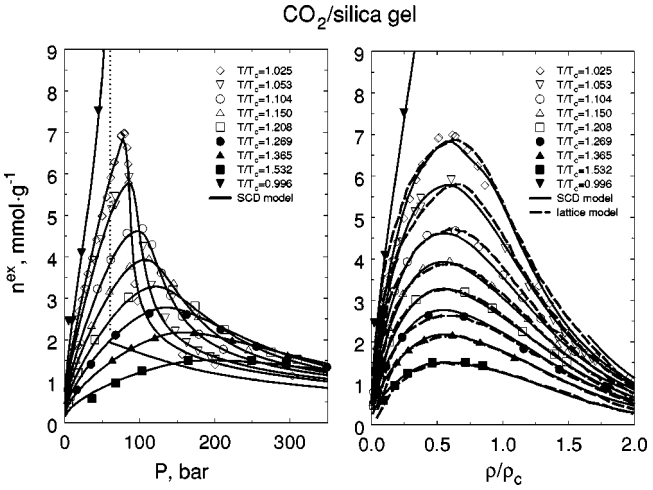

FIG. 16. Excess adsorption isitherms (Ref. 44) (symbols) of CO_2 on silica gel as functions of pressure (left) and density (right). The solid curves correspond to the values calculated with the SCD model and the dashed curves correspond to the values calculated with the lattice DFT model by Hocker *et al.* (Ref. 45). The dotted line represents the vapor pressure of pure bulk CO_2 calculated at $T=294$ K with the GCS EOS.

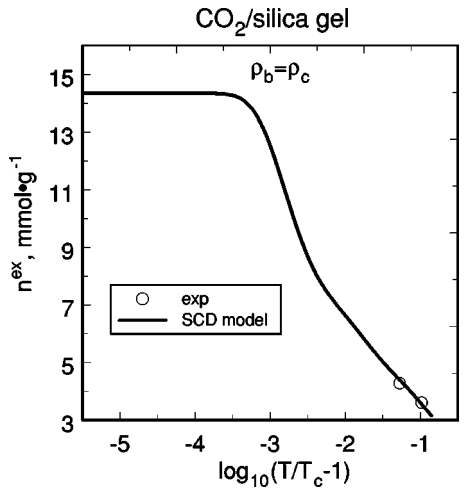

FIG. 17. Excess adsorption of CO_2 on silica gel along the critical isochore as a function of temperature. The symbols represent the experimental values (Ref. 44) and the curve corresponds to the values calculated with the SCD model.

therms measured by Di Giovanni *et al.*[44] are presented in the pressure and density variables, the SCD model predictions are also shown in Fig. 16 as functions of P and ρ. The dashed curves in Fig. 16 represent the values calculated for this system with the lattice DFT model by Hocher *et al.*[45] As one can see, in the supercritical region, at $T>T_c$, both the SCD and lattice DFT models give very similar predictions for the excess adsorption in the $T-\rho$ coordinates. However, unlike the lattice DFT model by Hocher *et al.*,[45] which was not applied at $T<T_c$, the predictions of the SCD model in the entire temperature range $0.996T_c \leqslant T \leqslant 1.532T_c$ are in excellent agreement with experimental all excess adsorption data by Di Giovanni *et al.*[44] in both $T-P$ and $T-\rho$ coordinates.

We should note that there is a fundamental difference between surface excess adsorption Γ and excess adsorption n^{ex} in a slit pore. In Fig. 17 we show the excess adsorption of CO_2 on silica gel along the critical isochore as a function of dimensionless temperature τ. As one can see, along the critical isochore the excess adsorption n^{ex} in the slit pores, unlike the surface excess adsorption Γ, does not decrease at $\tau \to 0$ but is monotonically increasing and saturating as the critical temperature is approached.

VI. CONCLUSION

In this work, we developed a generalized crossover density-functional theory model for critical adsorption in semi-infinite systems. Unlike the asymptotic crossover renormaliztion-group model developed earlier,[10] the GC DFT model not only reproduces the nonanalytic singular behavior of the excess adsorption in the critical region, but also can be extended to the dilute-gas and dense-fluid regimes. The GC DFT model has been justified by a direct comparison with all existing experimental excess adsorption data for Kr/graphite, C_2H_4/graphite, C_3H_8/griphite, CO_2/silica, and SF_6/graphite systems. For all systems, excellent agreement between theoretical predictions and experimental data in a wide range of the parameters of state, except the critical isochore data for SF_6/graphite system, has been achieved. The GC DFT model for the excess adsorption in a semi-infinite system, similar to the AC RG model,[10] fails to reproduce the ''critical depletion'' observed in experiment and attributed to the effect of confined geometry on the near-critical fluid.[15–17]

In order to overcome this shortcoming of the GC DFT model, we developed here a simplified crossover droplet model for the surface excess adsorption of pure fluids in a slit pore. The finite-geometry effect has been treated in the SCD model, as a density profile deformation, which appears in a slit pore when the size L of the pore becomes comparable with the correlation length of a bulk fluid ξ_b. In the large pore with $L \gg \xi_b$, the SCD model is transformed to the GC DFT model for a semi-infinite system. We realize that in a more rigorous theoretical approach the specific finite-scaling effects[16] and the dimensional renormalization of the effective critical exponents[46] from the three-dimensional values, at $L \gg \xi_b$, to the two-dimensional values, at $L \leqslant \xi_b$, should be taken into account. However, even in its present form, the simplified crossover droplet model does qualitatively explain a ''critical depletion'' of the excess adsorption observed in the SF_6/graphite system and yields an excellent quantitative description of all critical adsorption data obtained for this system and CO_2/silica gel system as well.

ACKNOWLEDGMENT

The research was supported by the U.S. Department of Energy, Office of Basic Energy Sciences, under Grant No. DE-FG03-95ER14568.

[1] D. Myers, *Surfaces, Interfaces, and Colloids. Principles and Applications*, 2nd ed. (Wiley-VCH, New York, 1999).
[2] P. C. Hiemenz, *Principles of Colloid and Surface Chemistry*, 2nd ed. (Dekker, New York, 1986).
[3] H. T. Davis, *Statistical Mechanics of Phases, Interphases, and Thin Films* (VCH, New York, 1996).
[4] B. Rangarajan, C. T. Lira, and R. Subramanian, AIChE J. **41**, 838 (1995).
[5] R. Subramanian, H. Pyada, and C. T. Lira, Ind. Eng. Chem. Res. **34**, 3830 (1995).
[6] R. Subramanian and C. T. Lira, in *Fundamentals of Adsorption*, edited by M. D. LeVan (Kluwer Academic, Boston, 1996).
[7] J. H. Chen, D. S. H. Wong, C. S. Tan, R. Subramanian, C. T. Lira, and M. Orth, Ind. Eng. Chem. Res. **36**, 2808 (1997).
[8] C. A. Croxton, *Liquid-State Physics—A Statistical Mechanical Introduction* (Cambridge University Press, London, 1974).
[9] H. Henderson, *Fundamentals of Inhomogeneous Fluids* (Dekker, New York, 1992).
[10] S. B. Kiselev, J. F. Ely, and M. Y. Belyakov, J. Chem. Phys. **112**, 3370 (2000).
[11] M. Thommes, G. H. Findenegg, and H. Lewandowski, Ber. Bunsenges. Phys. Chem. **98**, 477 (1994).
[12] M. Thommes and G. H. Findenegg, Langmuir **10**, 4270 (1994).
[13] M. Thommes, G. H. Findenegg, and M. Schoen, Langmuir **11**, 2137 (1995).
[14] M. Fisher and C. R. de Gennes, C. R. Seances Acad. Sci., Ser. B **287**, 207 (1978).
[15] M. Schoen and M. Thommes, Phys. Rev. E **52**, 6375 (1995).
[16] A. Maciolek, A. Ciach, and R. Evans, J. Chem. Phys. **108**, 9765 (1998).
[17] A. Maciolek, R. Evans, and N. B. Wilding, Phys. Rev. E **60**, 7105 (1999).
[18] N. B. Wilding and M. Schoen, Phys. Rev. E **60**, 1081 (1999).
[19] U. M. B. Marconi, Phys. Rev. A **38**, 6267 (1988).
[20] S. B. Kiselev, L. Lue, and M. Y. Belyakov, Phys. Lett. A **251**, 212 (1999).
[21] S. B. Kiselev, L. Lue, and M. Y. Belyakov, Phys. Lett. A **260**, 168 (1999).
[22] T. C. Lubensky and M. H. Rubin, Phys. Rev. B **12**, 3885 (1975).
[23] A. J. Bray and M. A. Moore, J. Phys. A **10**, 1927 (1977).
[24] H. W. Diehl, Int. J. Mod. Phys. B **11**, 3503 (1997).

[25] P. Upton, Phys. Rev. Lett. **81**, 2300 (1998).
[26] M. Fisher (private communication).
[27] S. B. Kiselev and J. F. Ely, J. Chem. Phys. **119**, 8645 (2003).
[28] G. F. Teletzke, L. E. Scriven, and H. T. Davis, J. Colloid Interface Sci. **87**, 550 (1982).
[29] J. S. Rowlinson and B. Widom, *Molecular Theory of Capillarity* (Clarendon, Oxford, 1982).
[30] J. V. Sengers and J. M. H. Levelt Sengers, Annu. Rev. Phys. Chem. **37**, 189 (1986).
[31] M. A. Anisimov and S. B. Kiselev, Sov. Technol. Rev. B **3**, 1 (1992).
[32] N. C. Patel and A. S. Teja, Chem. Eng. Sci. **37**, 463 (1982).
[33] N. C. Patel, Int. J. Thermophys. **17**, 673 (1996).
[34] J. Smukala, R. Span, and W. Wagner, J. Phys. Chem. Ref. Data **29**, 1053 (2000).
[35] G. H. Findenegg, in *Fundamentals of Adsorption*, edited by D. Myers and A. L. Belfort (Engineering Foundation, New York, 1983), p. 207.
[36] J. R. Strubinger and J. F. Parcher, Anal. Chem. **61**, 951 (1989).
[37] J. F. Parcher and J. R. Strubinger, J. Chromatogr. **479**, 251 (1989).
[38] S. B. Kiselev and J. F. Ely, Fluid Phase Equilib. (in press).
[39] A. V. Voronel (private communication).
[40] M. A. Anisimov, *Critical Phenomena in Liquids and Liquid Crystals* (Gordon and Breach, New York, 1991).
[41] L. D. Landau and E. M. Lifshitz, *Statistical Physics* (Pergamon, New York, 1980), pt. 1.
[42] A. Z. Patashinskii and V. L. Pokrovskii, *Fluctuation Theory of Phase Transitions*, 1st ed. (Pergamon, New York, 1979).
[43] J. V. Sengers and J. M. H. Levelt Sengers, in *Progress in Liquid Physics*, edited by C. A. Croxton (Wiley, Chichester, U.K., 1978).
[44] O. Di Giovanni, W. Dorfler, M. Mazzotti, and M. Morbidelli, Langmuir **17**, 4316 (2001).
[45] T. Hocker, A. Rajendran, and M. Mazzotti, Langmuir **19**, 1254 (2003).
[46] F. Freire, D. O'Connor, and C. R. Stephens, J. Stat. Phys. **74**, 219 (1994).
[47] D. R. Douslin and R. H. Harrison, Int. J. Thermophys. **8**, 301 (1976).
[48] P. Nowak, R. Kleinrahm, and W. Wagner, J. Chem. Thermodyn. **28**, 1441 (1996).
[49] N. B. Vargaftik, *Handbook of Physical Properties of Liquids and Gases*, 2nd ed. (Hemisphere, New York, 1983).
[50] K. C. Nadler, J. A. Zollweg, W. B. Streett, and I. A. McLura, J. Colloid Interface Sci. **122**, 530 (1988).